energies

MDPI

Article

Renewable Energy Communities in Islands: A Maltese Case Study

Alexander Micallef *, Cyril Spiteri Staines and John Licari

Department of Industrial Electrical Power Conversion, University of Malta, MSD 2080 Msida, Malta
* Correspondence: alexander.micallef@um.edu.mt

Abstract: Renewable energy communities are considered as key elements for transforming the present fossil fuel-based energy systems of islands into renewable-based energy systems. This study shows how renewable energy communities can be deployed in the Maltese context to achieve higher penetration of residential-scale photovoltaic systems. Case studies for five renewable energy communities in the Maltese LV distribution network have been analyzed in detail. A novel community battery energy storage sizing strategy was proposed to determine the optimal storage capacity at each energy community. The main objective of the community battery storage in each REC is to minimize the reverse power injection in the grid (minimize the total reverse energy and reverse peak power values), as well as to reduce the peak evening electricity demand. The optimal sizes for communal BESSs were determined to be of 57 kWh (EC 1), 55 kWh (EC 2), 31 kWh (EC 3), 37 kWh (EC 4) and 10 kWh (EC 5), respectively. The community storage systems were observed to reduce the overall impact of all five energy communities on the grid infrastructure. Power system simulations were performed for a typical spring day to evaluate the impact of communal BESS placement on the node voltages for all five energy communities. The results showed that the community storage was more effective at reducing the node rms voltage magnitudes when deployed at the end of the respective energy communities, rather than at the beginning of the community. During peak generation hours, reductions of up to 0.48% in the node rms voltage magnitudes were observed. This contrasts with reductions of only 0.19% when the community storage was deployed at the beginning of the energy communities.

Keywords: battery sizing; community storage; peak shaving; renewable energy community

Citation: Micallef, A.; Spiteri Staines, C.; Licari, J. Renewable Energy Communities in Islands: A Maltese Case Study. *Energies* **2022**, *15*, 9518. https://doi.org/10.3390/en15249518

Academic Editor: David Macii

Received: 29 November 2022
Accepted: 12 December 2022
Published: 15 December 2022

1. Introduction

The Renewable Energy Directive (2018/2001/EU) of the European Union (EU) [1] aims to make renewables more accessible to citizens, giving them the possibility to engage in joint renewable energy projects. The directive defines citizen-driven renewable energy communities (RECs) as legal entities that can produce, consume, store, and sell renewable energy or provide flexibility services to the grid through demand-response and storage.

Citizens are becoming increasingly environmentally and socially conscious towards energy issues. As a result, there is an increase in demand for more democratic processes in energy policies. Figure 1 summarizes the key elements of these RECs. RECs enable citizens to actively participate in the energy market through the deployment of community-scale storage and data obtained from second-generation smart meters [2]. The aggregation of participants in RECs is also advantageous to the distribution system operators (DSOs) as multiple flexible assets can be accessed through a single reference point. Recent literature on RECs has addressed issues related to the regulatory barriers [3–7], maximization of self-sufficiency [8–11], local energy sharing strategies [12–17] and the interaction of RECs with the power system [3,18].

1.1. Regulatory Challenges of RECs

Di Silvestre et al. [3] provide an in-depth analysis of the European REC experience, focusing on possible regulatory changes, together with technical and financial hurdles.

The authors analyze, in detail, the existing legislation and incentives set up in the EU member states in the wake of RED-II. An overview of the strengths of the RECs as a novel approach to energy management, as well as any critical issues related to their adoption, was also given. Ceglia et al. [4] define the social, economic and technical aspects of RECs, highlighting their advantages with respect to previous EU (and Italian) energy sharing directives. A case study for a REC in Benevento (Italy) was also described through data obtained from the HOMER database. The authors showed that RECs are more advantageous than conventional systems and systems of efficient users (SEU) on social and economic factors. Katsaprakakis et al. [5] provide a model for energy communities in Greek islands that aimed to achieve 100% energy self-sufficiency based on the lessons learned from existing Greek RECs in Sifnos, Crete, and Chalki. The case studies considered various elements, including general information about the existing Greek RECs, local power production (conventional and renewable), energy cooperatives and the Clean Energy transition agenda. The study by O'Neill-Carrillo et al. [6] identified possible practices that could overcome the technical and social challenges leading to the formation of RECs. The governance of the community was deemed as a fundamental pillar for the success of these communities. The three critical aspects that were identified are: sense of community, teamwork, and empowerment. Sense of community implies that any differences between the needs of the individual and the collective should not lead to conflicts within the community. Effective teamwork and coordination are critical to the success of the RECs. These aspects can only be reached if there is a set of rules that people agree on beforehand to collectively manage local resources. Empowerment enables citizens to have the proper tools to participate in the RECs, while ensuring that they are accountable for their decision-making and actions. Chamorro et al. [7] categorize RECs as being either Urban, Rural or Universities. Urban RECs are formed in cities, providing opportunities for sector coupling by combining energy, water, gas, and transportation services. Rural RECs provide inexpensive and reliable electricity supply to households and local businesses, which can also be isolated from the main grid. University RECs are typically living laboratories for green technologies as these emulate small cities. These simulated environments can provide ideal test sites for innovative technologies and management strategies.

1.2. Energy Optimisation Strategies for RECs

The maximization of self-sufficiency and self-consumption for prosumers is one of the most researched topics in literature. This is also the case when considering the integration of renewable energy sources and energy storage systems in RECs. Self-consumption (and self-consumption index KPI) defines how much of the local PV production is used locally, while the self-sufficiency (and self-sufficiency index KPI) defines the percentage of energy needs that the local generation can cater for. The authors of [8] developed a multi-variable optimization strategy that minimizes the energy provision costs for a representative REC in Flanders, Belgium. The mixed-integer linear model considers the electricity tariffs, the ratio of electrification of heating and transportation sectors, and the capital expenditure (CAPEX) of renewable energy sources and storage systems. The REC outperformed the other scenarios in the both the financial and environmental KPIs; however, the financial advantages over individual prosumers were not significant. This implies that for a wide adoption of RECs, citizens will need to be suitably incentivized. Similarly, Barone et al. [9] developed a multi-variable dynamic REC simulation model in TRNSYS and applied it to a case study in the island of El Hierro (Canary Islands, Spain). The simulation tool is aimed at achieving energy independence for remote islands, rather than focusing on its applicability to generalized objectives. A limitation of this study is that the solar PV generation was based on weather data from a nearby location, while the consumption data were obtained from real world data. Doroudchi, Khajeh and Laaksonen [10] maximize the self-sufficiency of RECs by introducing community and distributed storage to minimize the energy exchange with the utility grid. Excess generation from the community-owned solar PV generation is stored as thermal energy in both community scale and distributed

electric heat energy storage. The study showed that the payback period for the community scale storage is less than the distributed electric heat energy storage, even though the payback period depends on the usage. However, one should note that the sizing of the communal and distributed thermal storage was not a result of the problem formulation but was determined arbitrarily. Cielo et al. [11] proposed an optimization procedure to size community solar photovoltaic systems with integrated energy storage. The optimization procedure is based on the maximization of both self-consumption and self-sufficiency of the RECs. The sizing strategy is, however, heavily skewed towards economic REC models and frameworks. When applied to an Italian context, internal return rates of approx. 11% were obtained, highlighting the attractiveness of exploiting the REC concept.

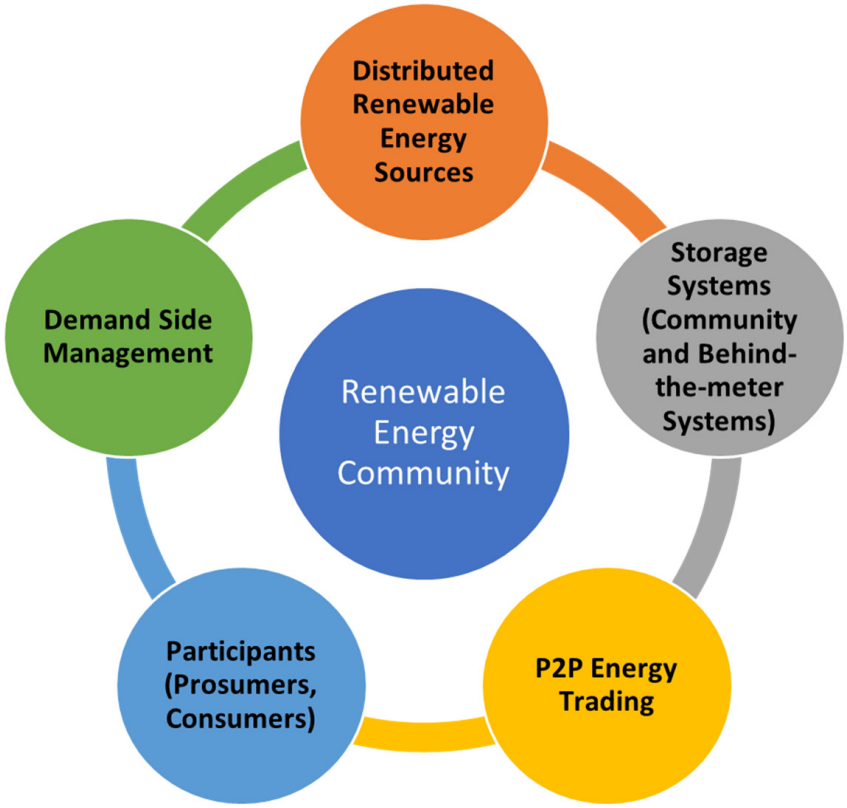

Figure 1. Block Diagram of the key elements in a Renewable Energy Community.

1.3. Citizen Driven Energy Markets

An important feature for RECs is the possibility of energy exchange between all the participants (utility, prosumers, and consumers). The authors of [12] proposed a local energy sharing strategy with a focus on price-forming methods. The proposed methods can be integrated into a net-billing system and adopted for different regulatory set-ups. This strategy can be used to improve local supply-demand balancing, reduce voltage deviations, and improve social welfare. However, the interactions and implications for the utility power system are not clear. Dolatabadi, Siano and Soroudi [13] proposed a real time optimization algorithm that preserves the privacy of prosumers within an REC. Similarly, Di Silvestre et al. [3] show how Blockchain technology can contribute to the development of RECs by enabling P2P energy trading with secure transactions while protecting personal data. The algorithm assesses the impact of energy exchanges within the community for the provision of ancillary services to the utility. The energy exchanges within the REC were considered as virtual self-consumption by the prosumers, together with the provision of ancillary services. However, this strategy would limit the market participation by consumers that cannot own local renewables and/or storage systems. The authors of [14] proposed a peer-to-peer (P2P) energy trading system for RECs that would

enable each prosumer to manage their energy consumption, storage scheduling and energy trading. The proposed community-based P2P energy trading system combines an online energy control with a double auction trading algorithm. The authors of [15,16] consider the scheduling of community energy storage to maximize the usage by all consumers while accounting for operational constraints. The scheduling heuristic makes use of a day-ahead auction approach to share the resources within the REC by making use of a time-of-use (TOU) tariffs. Aziz, Dagdougui and Elhallaoui [17] applied mean field game theory to determine Nash equilibrium strategies for an REC that includes 100 prosumers (with solar photovoltaic systems), located in Montreal city. The REC is formed through a virtual power bank that contains the distributed BESSs of the prosumers. The solutions for the community microgrid optimization minimize household individual cost functions and, in turn, reduces the aggregate cost by at least 40%.

1.4. Interaction of RECs with the Main Grid

While there are several studies analyzing the interaction of integrating battery energy storage at utility level (high-voltage and medium-voltage) with the utility grid, the topic of how RECs affect the electricity network has not yet received due attention in the literature [3]. The integration of storage at utility level (high-voltage and medium-voltage) is beyond the scope of this study, as RECs in the Maltese context are being envisaged at the LV network. The authors of [3] discuss how the formation of RECs will impact present interactions of prosumers with the electric power system by focusing on the Italian scenario. The authors also raised a number of questions, that remain to be addressed, for the effective integration of RECs into power systems, including the number of points of common coupling (PCC) with the main grid, the assessment of the impact on the main grid, the capability to provide ancillary services, and the capability to support the widespread adoption of demand response, amongst others. Sudhoff et al. [18] consider the reduction in the peak power exchange between the community and the electric grid through the prosumer PV and battery systems, together with flexible loads. A case study comparing rural, urban, and suburban RECs showed that the establishment of RECs resulted in less energy being required from outside the community. The study also shows that there is no minimum REC size to offer ancillary services to the grid using the local available assets.

1.5. Renewables in the Maltese Islands

The penetration of renewable energy sources in Malta has been increasing over the years, despite the demographic and spatial limitations of the Maltese islands. During 2021, 9.9% of the electricity supply in Malta was obtained from renewable sources (mainly photovoltaics). The domestic sector accounted for 93.6% of the total stock of solar photovoltaic (PV) installations and 46.1% of the total energy production [19]. The scenario depicted in Figure 2 compares the present Maltese RES share to that of other EU countries. However, the challenges that must be overcome to achieve higher penetrations of RES in the Maltese distribution network should not be taken lightly. The RECs provide an attractive solution to overcome some of the existing challenges.

The rest of the paper is organized as follows. Section 2 describes the methodology used for the study reported in this paper. Section 3 contains a description of the five considered renewable energy communities in the Maltese LV distribution network. Section 4 describes the proposed battery sizing strategy that determines the minimum BESS based on the defined battery utilization factor (BUF). Section 5 describes a case scenario for the five RECs on a typical spring day, showing the impact of the placement of the communal BESS on the voltage profiles of the energy communities. A summary of the obtained simulation results is given in Section 6 on the implications of this study.

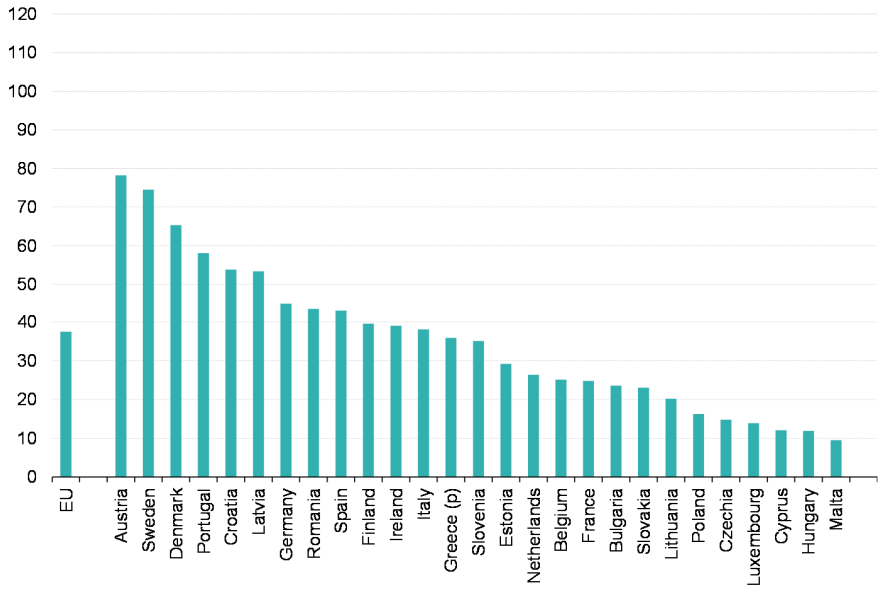

Figure 2. Share of Energy from Renewable Sources in the EU in Gross Electricity Consumption. Source: Eurostat (online data code: nrg_ind_ren).

2. Methodology

This study shows how RECs could be deployed in the Maltese context to improve the penetration of RES. The centralized community storage in the RECs was aimed at increasing the self-sufficiency of the RECs. In addition, the reduction in the peak electricity demand and minimization of the reverse power flows into the utility grid was also addressed. This study also proposes a community-scale battery energy storage system (BESS) sizing strategy, based on the battery utilization factor. This strategy was previously evaluated by the authors of [20] for utility scale storage and adapted to community scale applications. The methodology used in this paper is summarized in Figure 3. The workflow is subdivided into three main parts as follows:

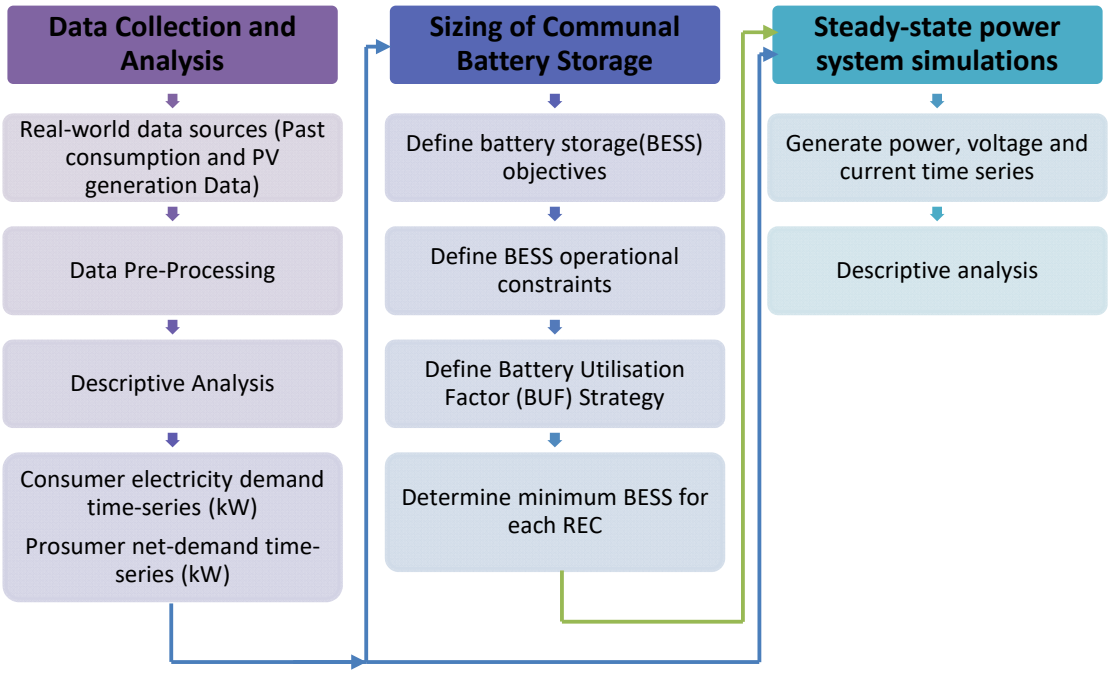

Figure 3. Methodology applied in this study to analyze the potential of RECs in reducing the reverse power flows and reducing the evening peak demand.

(1) collection and analysis of consumption and PV generation data (Section 3)

During the initial stages, the topologies for renewable energy communities in the Maltese context were defined. Data collection and the analysis of the real-world consumption and PV generation data were performed. The aggregated results grouped according to each respective REC are summarized in the next section.

(2) sizing of communal battery storage systems (BESSs) (Section 4)

The historical electricity consumption and PV generation data were used as an input to the battery utilization factor (BUF) sizing strategy. The BUF was used to determine the minimum BESS for each respective REC for the functionality and operational constraints described in this study.

(3) power system simulations to show RECs can improve the local voltage profiles (Section 5)

Steady-state power system simulations for a typical Maltese spring day were then used to produce the voltage profiles of each respective REC. The consumer and prosumer electricity net-demand profiles specify the net active power across each node in the REC, except at the substation transformer. A power-flow solution was implemented in MATLAB/Simulink to obtain the node voltages of each REC, over a 24 h period and with a 15 min resolution.

Problem Formulation and Constraints

As has been defined in the previous sections, the main objective of the community BESS in each REC is to minimize the reverse power injection in the grid (minimize the total reverse energy and reverse peak power values), as well as to reduce the peak evening electricity demand. Therefore, the objective of the communal BESSs aims to minimize the power losses at the PCC of each REC. The objective function can be defined by:

$$P_{loss} = \min\left\{\sum_{t=1}^{t_{total}} \sum_{i,j=1,i\neq j}^{n_t} g_{i,j}\left(V_i^2 + V_j^2 - 2\,V_i V_j \cos\left(\theta_i - \theta_j\right)\right)\right\} \quad (1)$$

where t is the time interval; t_{total} = 96 is the total time period (with 15 min resolution); $g_{i,j}$ is the conductance between buses i and j; n_t is the total number of branches in the REC; V_i and V_j are the voltage magnitudes of the buses i and j; and θ_i and θ_j are the voltage angles of buses i and j.

The BESS systems were sized according to the methodology defined in Section 4. The following assumptions and constraints were considered for the BESS sizing and the analysis carried out in the next sections:

- The power balance equation at the PCC of each REC is defined by:

$$\mathrm{P}_t^{\mathrm{grid}} = \mathrm{P}_t^{\mathrm{netload}} + \mathrm{P}_t^{\mathrm{charge,BESS}} - \mathrm{P}_t^{\mathrm{discharge,BESS}} \quad (2)$$

  where $\mathrm{P}_t^{\mathrm{grid}}$ is the power from/to the grid; $\mathrm{P}_t^{\mathrm{netload}} = \mathrm{P}_t^{\mathrm{distrbutedPV}} - \mathrm{P}_t^{\mathrm{distirbutedLoad}}$ is the difference between the distributed PV generation and the load consumption; $\mathrm{P}_t^{\mathrm{charge,BESS}}$, $\mathrm{P}_t^{\mathrm{discharge,BESS}}$ are the power charged and discharged by the BESS.
- The BESS round-trip energy efficiency consisting of the battery charging and discharging efficiencies (includes that of the power electronic converter) is assumed constant at 85%. The efficiency of the power electronic converter is assumed to remain constant for any output power from the BESS. Therefore, the charging efficiency, $\eta^{\mathrm{charge,bess}}$, is of 92.2% and the discharging efficiency, $\eta^{\mathrm{discharge,bess}}$, is of 92.2%.
- The BESS SoC is constrained to within the range between an $\mathrm{SoC}_t^{\mathrm{min,bess}}$ of 20% and an $\mathrm{SoC}_t^{\mathrm{max,bess}}$ of 80% to prolong the lifetime, i.e.:

$$\mathrm{SoC}_t^{\mathrm{min,bess}} \leq \mathrm{SoC}_t^{\mathrm{actual,bess}} \leq \mathrm{SoC}_t^{\mathrm{max,bess}} \quad (3)$$

  where $\mathrm{SoC}_t^{\mathrm{actual,bess}}$ is the actual battery SoC at any time of the day.

- The BESS useable energy capacity is constrained to use the energy available within the range as defined by the SoC constraints, i.e.:

$$E_t^{min,bess} \leq E_t^{actual,bess} \leq E_t^{max,bess} \quad (4)$$

where $E_t^{actual,bess}$ is the available battery energy at any time of the day.

- The maximum discharge power $P_t^{discharge,bess}$ was limited to a maximum value of 1C ($P_{MAX}^{discharge,bess}$):

$$P_t^{discharge,bess} \leq P_{MAX}^{discharge,bess} \quad (5)$$

- The maximum charging power $P_t^{charge,b}$ was limited to a maximum value of $P_{MAX}^{discharge,bess}$:

$$P_t^{charge,bess} \leq P_{MAX}^{charge,bess} \quad (6)$$

- The actual energy stored in the BESS, $E_t^{Actual,bess}$, is determined by adding the net-energy of the BESS in the previous time step, $E_{t-1}^{Actual,bess}$, to the energy charged in the BESS, $E_t^{charge,bess}$, and subtracting the discharged energy, $E_t^{discharge,bess}$. The energy conservation equation of the BESS is defined by:

$$E_t^{Actual,bess} = E_{t-1}^{Actual,bess} + E_t^{charge,bess} - E_t^{discharge,bess} \quad (7)$$

- The peak shaving operation is only functional if the evening maximum demand $P_t^{demand,REC}$ at the grid operators PCC exceeds the pre-defined maximum limit of the respective REC. In these cases, the BESS discharges to reduce the peak demand according to the available energy in the BESS:

$$P_{MAX}^{demand,REC} \leq P_t^{demand,REC} \quad (8)$$

- The BESS is assumed to be discharged at the start of the analysis (initial SoC of 20%).
- The self-discharge rate was considered negligible.
- Other battery-specific characteristics were not considered.

3. Energy Communities in a Maltese Context

Figure 4 shows the simplified line diagram of a typical secondary substation in the Maltese LV distribution network. The substation has 182 nodes, with 192 single-phase consumers and 14 three-phase consumers. The consumers are divided across five feeders connected to the secondary (LV) side of a 250 kVA, 11,000/400 V, 50 Hz, Dyn11 substation transformer with off-load tap changer. The off-load tap setting is set to −5%, such that the voltage levels at the end of the feeders have a suitable voltage level all year round. The effective turns ratio is set to 10,450/400 V to satisfy the limits defined in the Enemalta Network Code [21].

RECs at a LV network level can take various shapes and sizes. In this study, it is assumed that the energy community (EC) configurations are a direct result of how the consumers are presently connected to the LV network. Each LV feeder was considered as a separate REC. In this way, RECs can be formed without the need to reconfigure the present distribution network. Therefore, each EC consists of different combinations of single-phase and three-phase consumers/prosumers.

The distribution of the customers connected at each feeder is given in Table 1. The net-demand profiles for each of the single-phase and three-phase consumers were obtained from the local DSO in the form of a single spreadsheet for a one-year period (from 1 May 2020 to 31 April 2021) with a 15-min time resolution. Table 1 additionally shows the subset of consumers that also have a functional residential-scale PV system installed (i.e., the prosumers in the RECs). The PV generation profiles for each of the residential-scale PV

systems were also obtained in the same format from the local DSO. An important limitation is that most of the single-phase main meters did not have any logs for the exported active power. Therefore, the relationship between the PV generation and exported active power had to be analyzed and approximated for each individual consumer. The single-phase PV systems installed capacities range between systems of 1.38 kWp and 4.38 kWp, while the three-phase PV systems range between 1.84 kWp and 10.8 kWp. The total installed PV capacity in each of the RECs are as follows: 52.72 kW (REC 1), 48.56 kW (REC 2), 37.87 kW (REC 3), 29.07 kW (REC 4) and 12.78 kW (REC 5).

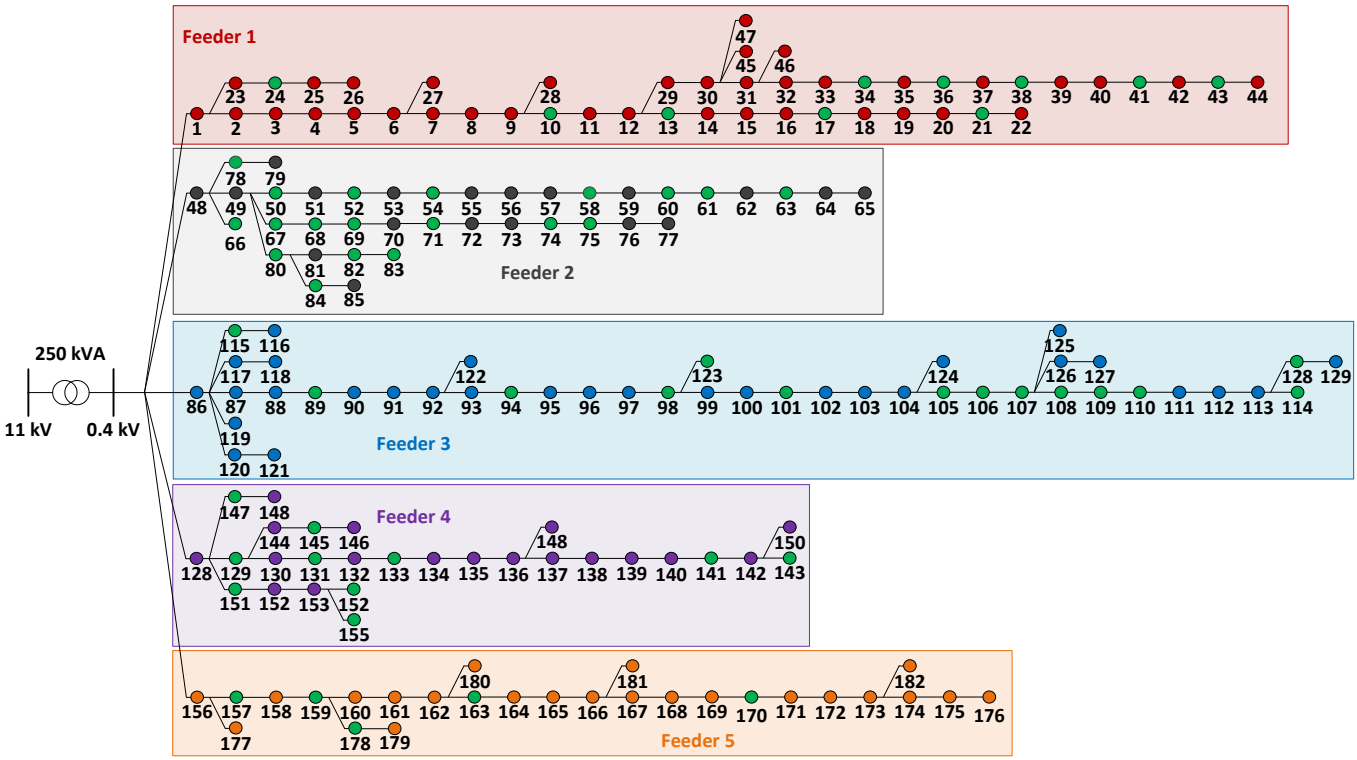

Figure 4. Simplified line diagram of the LV network at secondary substation. Feeder nodes are color coded for ease of reference (Red—Feeder 1, Black—Feeder 2, Blue—Feeder 3, Purple—Feeder 4, Orange—Feeder 5). Nodes where PV systems are connected are shown in green. Substation transformer is showing the nominal ratio without the off-load tap changer settings. The numbers in the figure identify the individual nodes of the LV network.

Analysis of the Net-Demand

Figure 5 illustrates the daily net-demand curves for each of the RECs. The estimated REC net-demand characteristics were determined from the data measured by the smart meters installed at the respective consumers/prosumers. This estimate of the total net-demand per REC gives a good approximation but it does not consider the distribution losses. Detailed analysis of the daily net-demands of all five RECs shows that oversupply occurs on more than 340 days for RECs 1 to 4, while for REC 5, oversupply occurs on 265 days. Oversupply was always observed to occur during the middle of the day as this coincides with the peak of PV generation.

One of the primary concerns resulting from the reverse power flow is the significant voltage rise that can occur along the feeder. The feeder voltage could potentially increase enough to violate the ±10% steady state tolerance defined in the Enemalta network code [21]. The voltage levels of the other feeders in the LV network can also be affected by the reverse power flowing back to the substation transformer. An additional concern is that, on a larger scale, the reverse power flow could lead to dynamic stability issues. During

instances of reverse power, there is a lack of system inertia, which is an issue when coupled with the intermittency risks associated with PV generation.

Table 1. Consumers and PV systems connected to the secondary substation LV network.

		Single-Phase		Three-Phase		Maximum Feeder Lengths
REC (Feeder)	Phase	Consumers	PV Systems	Consumers	PV Systems	
1	A B C	10 12 19	4 4 2	9	3	542.466 m
2	A B C	12 15 9	7 6 5	1	-	221.6 m
3	A B C	16 25 17	4 7 2	3	1	623.16 m
4	A B C	5 12 13	2 3 4	1	1	302.074 m
5	A B C	1 13 13	- 4 1	-	-	621.852 m

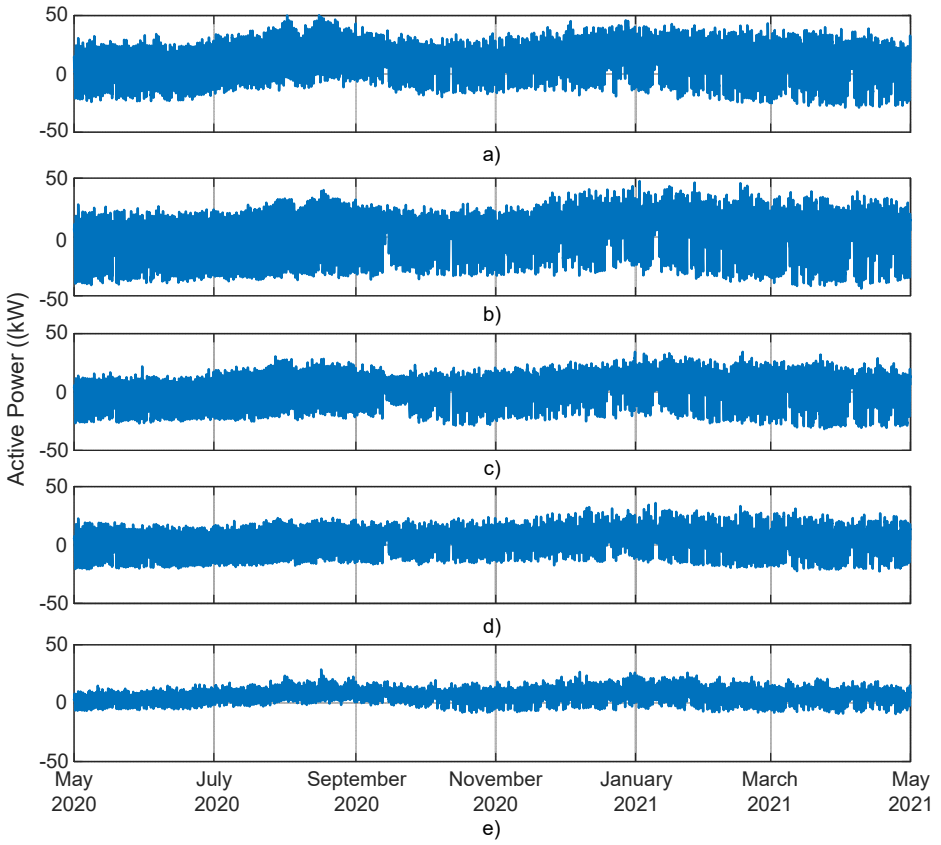

Figure 5. Daily Net-Demand Curve for each of the eCs during the considered period. (**a**) EC1 (Feeder 1). (**b**) EC2 (Feeder 2). (**c**) EC3 (Feeder 3). (**d**) EC4 (Feeder 4). (**e**) EC5 (Feeder 5). Positive active power values for the net-demand represent the power consumption by the consumer loads while negative active power values represent the reverse power flow due to the local PV generation.

One must note that this study was performed during the COVID-19 pandemic. The COVID-19 pandemic has affected every aspect of life, including the operation of the utility grid due to changes in the energy usage patterns of residential, commercial, and public entities. According to a study published by the Malta National Statistics Office [19], the total electricity supplied in 2020 amounted to 2496.4 GWh, which is a decrease of 5.4% when compared to the previous year.

4. Community BESSs for the RECs

Community battery energy storage systems (BESSs) have a typical storage capacity ranging between tens of kilowatt-hours (kWh) and a few megawatt-hours (MWh). BESSs are an effective and energy efficient solution to limit reverse power flows in the LV distribution network. The community-scale BESSs can be sized according to a wide variety of site performance requirements. In this paper, the community-scale BESSs are deployed at specific nodes in the REC and controlled to reduce the power exchanges with the medium voltage network (11 kV). Two locations for the integration of BESS into the RECs were investigated in this study: at the start of the REC and at the end of the REC. Figure 6 shows an example of the possible locations that were identified for EC5. These siting constraints were imposed by the typical densely populated Maltese towns/villages that do not enable the deployment of central community BESSs at the intermediate nodes.

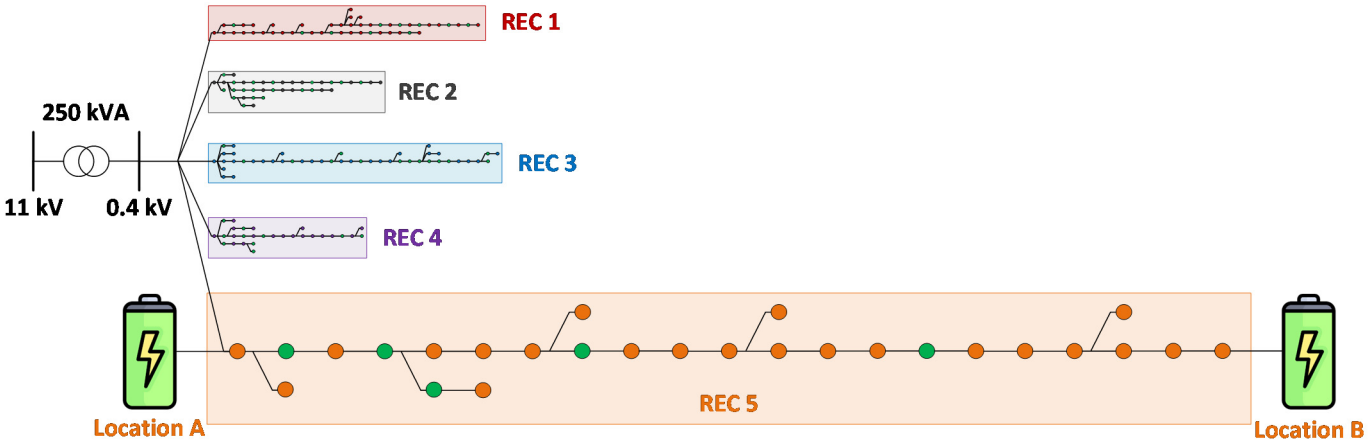

Figure 6. Possible locations for Centralized Community Storage Systems for EC5. Location A is the start of the REC. Location B is at the end of the REC.

4.1. Community BESS Sizing Strategy

Sizing strategies that are available in the literature typically result in a trade-off between the near-term cost and long-term technical complexity. In this study, the battery utilization factor (BUF), previously defined in [20], was used to size the BESSs at each respective REC. The BUF is determined by the daily variations in the state of charge (SoC) (i.e., cycling of the BESSs) as the BESS operates daily to minimize the power exchanged with the grid. The daily variations in the SoC of the BESSs is affected by the operating conditions, including the charge and discharge rates, depth of discharge, cycle duration, and length of time in the standby mode [20]. The BUF for the community-scale BESS at each respective REC can be defined by:

$$\mathrm{BUF} = \frac{\sum_{n=1}^{365} \left(\frac{W_1 T_{\mathrm{Charge}_n}}{T_{\mathrm{ReversePower}_n}} \right) \left(\frac{W_2 T_{\mathrm{Discharge}_n}}{T_{\mathrm{PeakDemand}_n}} \right)}{\text{Number of days}} \tag{9}$$

where n = 1, . . . , 365 are the days over the considered period; W_1 is the weighting during the charging periods based on the daily SoC variations during charging; W_2 is the weighting during the discharging periods based on the daily SoC variations during discharging. The

daily charging duty cycle for the nth day is defined as the ratio of the actual charging time (T_{Charge} in minutes) to the reverse power flow duration ($T_{ReveresePower}$ in minutes). T_{Charge} is defined as the time duration required to charge the battery to full capacity each day while $T_{ReveresePower}$ is the daily time interval during which reverse power flows back to the substation transformer. The daily discharging duty cycle for the nth day is defined as the ratio of the actual discharging time ($T_{Discharge}$ in minutes) to the duration of the EC evening peak ($T_{PeakDemand}$ in minutes). $T_{Discharge}$ is the daily time duration required to discharge the battery to the minimum SoC while $T_{PeakDemand}$ is the time interval during which the maximum power at the EC exceeds the pre-set daily limit.

4.2. BUF and Optimal Community BESS (Present PV Penetrations)

The flowchart in Figure 7 describes the BESS sizing procedure. The BUF calculation, as defined in (9), was used as a discrete computational procedure to determine the optimal BESS solution for each of the RECs. The BESS optimization process for the RECs is independent of the objective function being optimized. This was conducted by initially defining for each REC: $P_{MAX}^{charge,bess}$; the lower BESS capacity bound, C_{MIN}^{bess}; an upper BESS capacity bound, C_{MAX}^{bess}; and the number of iterations by the step size, C_{step}^{bess}. The evaluated BESS capacity, C_x^{bess}, is initially set to the lower capacity bound and the BUF is determined by the methodology shown in Figure 7. The C_x^{bess} is then incremented with each iteration of the BUF algorithm. Each iteration gives a BUF point on the curve that can be plotted on a BUF vs. BESS capacity curve. An example of the BUF vs BESS capacity curve is shown in Figure 8. The maxima resulting from this curve yields the BESS capacity with the maximum utilization factor. Due to the weighted formulation of (9), there can only be one maximum for each BUF vs BESS capacity curve. The BUF was determined for BESS systems rated between 1 kWh and 200 kWh (in steps of 1 kWh) at a $P_{MAX}^{charge,bess}$ of 0.1C up to 0.5C (in steps of 0.1C). The resulting BUF vs BESS capacity curves are shown in Figure 8. The $P_{MAX}^{demand,REC}$ daily maximum power limits for each respective REC were set as a constant throughout the entire year according to the pre-determined thresholds for the daily peak demands at each EC. These were determined to be 10 kW (EC1 to EC4) and 7 kW (EC5), respectively.

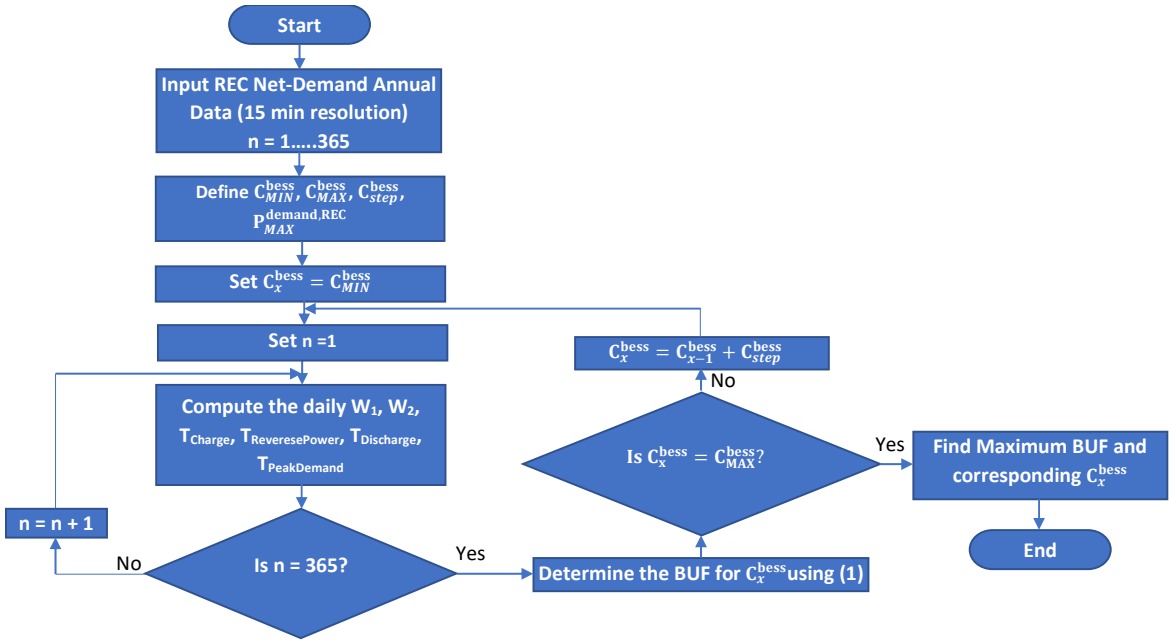

Figure 7. Flowchart of the BESS sizing procedure using the BUF Strategy (n = 1, . . . , 365 is the day number.

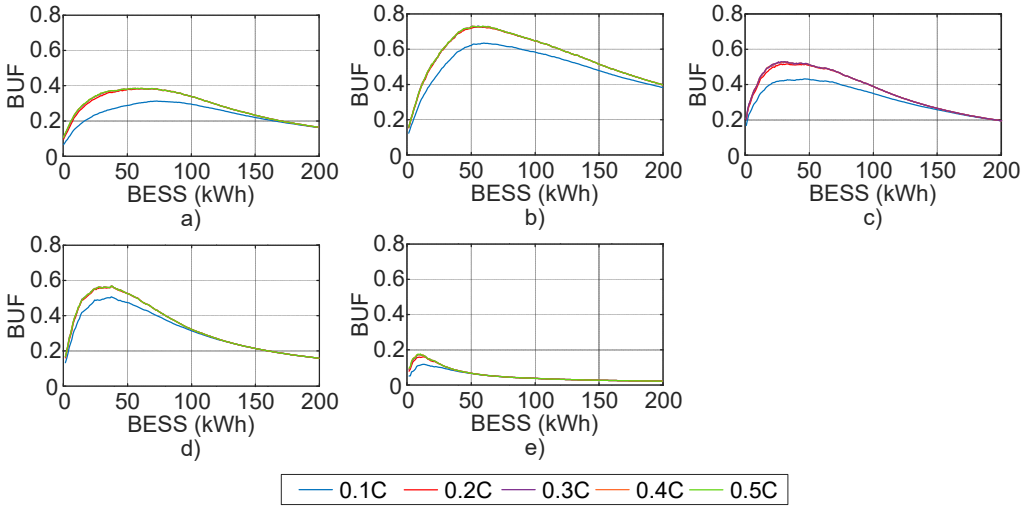

Figure 8. Battery Utilization Factor for BESS systems rated from 1 kWh to 200 kWh at charging rates of 0.1C up to 0.5C. (**a**) BUF for EC 1. (**b**) BUF for EC 2. (**c**) BUF for EC 3. (**d**) BUF for EC 4. (**e**) BUF for EC 5.

An analysis of Figure 8 reveals that the BUF characteristic are directly dependent on the daily net-demand characteristics (including the reverse power flows and peak evening load demands). In all of the RECs, the BUF was observed to be affected by low values of $P_{MAX}^{charge,bess}$, with the worst performance occurring at 0.1C. However, the improvements observed in the BUF for $P_{MAX}^{charge,bess}$ above 0.3C were negligible. The lowest BUF from all ECs can be observed at EC5 as the BESS can only charge during the reverse power periods. If the peak load demand does not exceed the threshold, the BESS does not discharge, resulting in extended periods of idle time. The highest BUF was observed for EC2 that has high reverse power flows and peak demands that are of similar magnitudes. The optimal sizes for communal BESSs (at a charging rate of 0.3–0.5C) were determined to be of 57 kWh (EC 1), 55 kWh (EC 2), 31 kWh (EC 3), 37 kWh (EC 4) and 10 kWh (EC 5), respectively.

4.3. Energy Community Net Demand with BESSs

The hourly net-demand curves for the each of the RECs with the addition of community storage are considered in this section. Only the results obtained with the determined $BESS_{BUF}$ are given in this section for each of the RECs. For EC1, additional results were included for a BESS twice the optimal value to compare the operational performance. The simulations were performed to evaluate the impact of the $BESS_{BUF}$ on the reverse power flow and total energy demand at each REC. In addition, the daily SoC variations for the community scale BESS are also given.

4.3.1. Energy Community 1

Figure 9a shows the hourly net-demand curves with and without the $BESS_{BUF}$ of 57 kWh (showing the average power over 15-min intervals in kW), together with the daily SoC for EC1 over the considered year. The total energy demand in the EC without storage is of 111.3 MWh, while the total energy flowing back to the substation amounts to 17.5 MWh. The total energy demand in the EC with $BESS_{BUF}$ is of 102.98 MWh, while the total energy flowing back to the substation amounts to 8.19 MWh. The BESS is not large enough to eliminate the reverse power flows on most days. One can observe that the BESS is cycled nearly daily between the predefined SoC limits. An exception occurs in the period between mid-July and mid-September due to lower magnitudes of reverse power flow resulting from higher electricity demands. In addition, one can also observe that the BESS does not always have sufficient energy to limit the evening peak demand to the pre-defined set point.

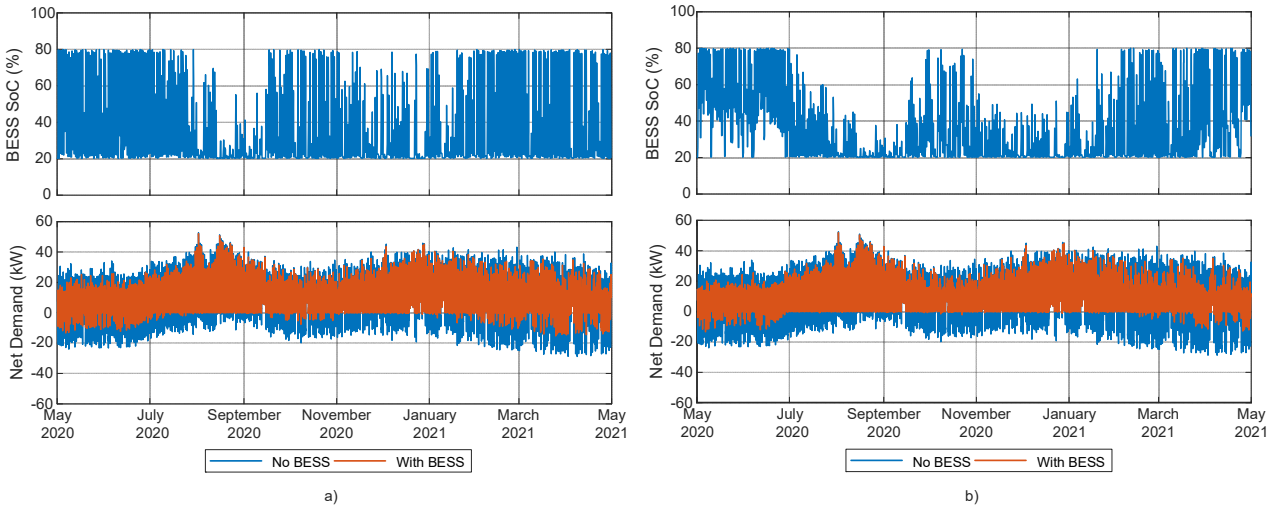

Figure 9. Net demand with and without storage and daily variations in the State of Charge for EC1. (**a**) With a 57 kWh BESS. (**b**) With a 114 kWh BESS.

Increasing the size of the BESS to 114 kWh results in further reductions of the reverse power flow. With this larger BESS, the total energy flowing back to the substation reduces to 4.66 MWh. The total energy demand reduces to 99.7 MWh as more energy was supplied by the BESS during peak shaving operation on most days where the demand exceeded the defined set-point. Figure 9b shows the hourly net-demand curves with and without storage, together with the SoC variations for EC1. The BESS works in daily microcycles on days where: (a) the absorbed reverse power flow exceeds the discharged energy during the evening peak demand periods; and (b) the absorbed reverse power flow is much less than the evening peak demand periods. While these microcycles have the advantage of increasing the lifetime of the battery, this comes at significantly higher capex and spatial footprint requirements. The latter is an extremely critical aspect due to the densely built Maltese environment, which limits the deployment of distributed large-scale BESSs.

4.3.2. Energy Community 2

Figure 10a shows the hourly net-demand curves with and without the $BESS_{BUF}$ of 55 kWh (average power over 15-min intervals in kW), together with the SoC variations for EC2, over the entire year. The total energy demand in the EC without storage is of 77.23 MWh, while the total energy flowing back to the substation amounts to 52.3 MWh. The total energy demand in the EC with $BESS_{BUF}$ is of 67.47 MWh (reduction of 12.64%), while the total energy flowing back to the substation amounts to 41.47 MWh (reduction of 20.7%). One can observe that the BESS is cycled nearly daily between the predefined SoC limits, except in the period between May and July, when the electricity demand was low and the PV generation was high. However, the BESS is not large enough to eliminate the reverse power flows on all days. In addition, the BESS does not always have sufficient energy to limit the evening peak demand to the pre-defined set point.

4.3.3. Energy Community 3

Figure 10b shows the hourly net-demand curves with and without a 31 kWh BESS (average power over 15-min intervals in kW), together with the SoC variations for EC3, over the considered period. The total energy demand in the EC without storage is of 59.65 MWh, while the total energy flowing back to the substation amounts to 32.78 MWh. The total energy demand in the EC with $BESS_{BUF}$ is of 55.2 MWh (reduction of 7.46%), while the total energy flowing back to the substation amounts to 27.8 MWh (reduction of 15.19%). One can observe that the BESS is cycled nearly daily between the predefined SoC limits, except in the period between early-May and the end of June, when the daily maximum electricity demand is very close to the defined setpoint. However, the BESS is not large enough to

eliminate the reverse power flows on all days. In addition, the BESS does not always have sufficient energy to limit the evening peak demand to the pre-defined set point.

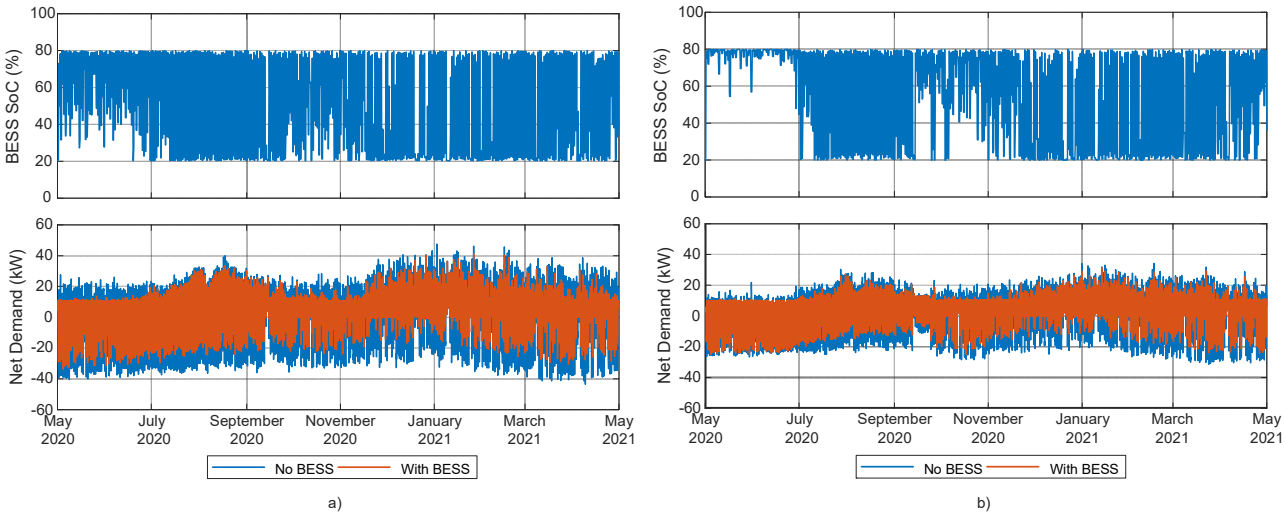

Figure 10. Net demand with and without storage and daily variations in the State of Charge. (**a**) EC2 with a 55 kWh BESS. (**b**) EC3 with a 31 kWh BESS.

4.3.4. Energy Community 4

Figure 11a shows the hourly net-demand curves with and without a 37 kWh BESS (average power over 15-min intervals in kW), together with the SoC variations for EC4, over the considered period. The total energy demand in the EC without storage is of 56.01 MWh, while the total energy flowing back to the substation amounts to 23.42 MWh. The total energy demand in the EC with $BESS_{BUF}$ is of 50.75 MWh (reduction of 9.39%), while the total energy flowing back to the substation amounts to 17.57 MWh (reduction of 25%). One can observe that the BESS is cycled nearly daily between the predefined SoC limits, except in the period between the beginning of May and mid-July. From Figure 11a, one can observe that the BESS is effective in limiting the maximum demand to the required reference of 10 kW for all days in this period. In this EC, the BESS is not large enough to eliminate the reverse power flows on all days. In addition, the BESS does not always have sufficient energy to limit the evening peak demand to the pre-defined set point, except in the period between the beginning of May and mid-July.

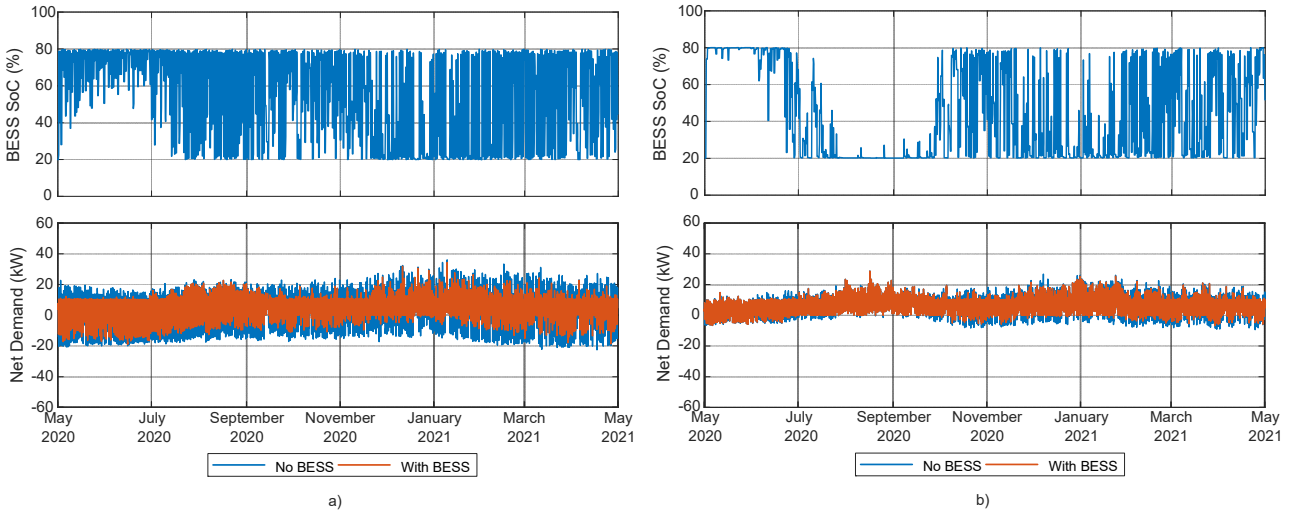

Figure 11. Net demand with and without storage and daily variations in the State of Charge. (**a**) EC4 with a 37 kWh BESS. (**b**) EC5 with a 10 kWh BESS.

4.3.5. Energy Community 5

Figure 11b shows the hourly net-demand curves with and without a 10 kWh BESS (average power over 15-min intervals in kW), together with the SoC variations for EC5, over the considered period. The total energy demand in the EC without storage is of 55.05 MWh, while the total energy flowing back to the substation is the lowest of all ECs, at 2.78 MWh. The total energy demand in the EC with $BESS_{BUF}$ is of 54.3 MWh (reduction of 1.36%), while the total energy flowing back to the substation amounts to 1.94 MWh (reduction of 30.2%). Even though the size of the BESS is small, the BESS is underused throughout the entire year. During May and June, the electricity demand is lower than the maximum threshold, resulting in the BESS operating at the maximum SoC of 80%. Hence, the BESS could not reduce the reverse power flows during this period. In the late summer months, the electricity demand increases due to the cooling requirements (air-conditioning loads). This results in no reverse power flow and, hence, the BESS operates at the minimum SoC of 20%. Therefore, one can clearly conclude that the BESS was underused between May and September 2020. Between October 2020 and April 2021, the reverse power flows and the evening peak demands were reduced as the BESS was cycled on a frequent basis. Increasing the size of the BESS to values higher than the $BESS_{BUF}$ at the present levels of PV generation would yield even further underutilization. Assuming that the electricity demand of REC5 does not increase, energy independence from the utility grid can be achieved by increasing both the PV generation and the BESS size.

5. Case Study: Typical Maltese Spring Day

The secondary substation distribution network shown in Figure 4 was modelled in MATLAB/Simulink. The cables and overhead lines were represented as distributed Pi-transmission line models. Technical data on each cable segment included the cable type per segment, segment lengths, and the electrical parameters per unit length (resistance, inductance, and line-to-ground capacitance) were provided by the local DSO to achieve a detailed schematic. These detailed cable parameters are critical to evaluating the effects of high periods of PV generation on the node voltage profiles of each energy community.

Electrical parameters of the secondary substation transformer were also included for these simulations. The primary side of the substation transformer acts as the slack bus to balance the active power and reactive power in the modelled network. This bus acts as a reference to the simulation model and is the only known voltage at the start of the simulation. Single-phase and three-phase load buses were implemented at each node to model the respective consumer loads and local PV generation.

Power flow simulations were carried out for two grid placement scenarios to evaluate the impact of communal BESS placement on the node voltages of all five energy communities. The first location is at the start of the feeder (Location 1) as the BESSs can be located within the substation or in its vicinity (i.e., the most accessible location). The second location is at the end of the feeder (Location 2), where the reduction in the energy community node rms voltages is expected to be more significant. However, in practice, there might be practical limitations that could not allow the deployment of communal BESSs at Location 2 (refer to Section 5).

5.1. Spring Net-Demand Characteristics

Spring is the best performing season for PVs in Malta due to a combination of cooler ambient temperatures, low electricity demand for heating/cooling, high irradiation levels and high levels of sun-hours [20]. On the other hand, winter has a higher electricity demand resulting from space/water heating and the lowest levels of sun hours, when compared to the other seasons.

The hourly net demand curves without community BESS for 8 May 2020 are shown in Figure 12. One can observe that the net demand curves for all ECs on this day follow the duck curve characteristic. Oversupply occurs during the middle of the day, as this coincides with the peak of PV generation. This negative net-demand occurs between, approximately,

8 am and 6 pm for all ECs. EC2 has the highest reverse power of all the ECs at −23.8 kW, with the reverse peak being twice the evening peak demand.

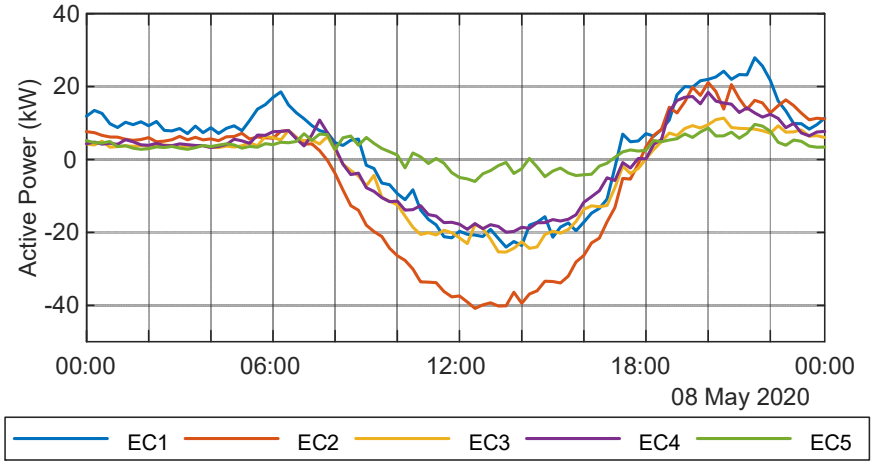

Figure 12. The hourly net demand curves for all ECs on 8 May 2020.

5.2. EC Net-Demand Characteristics with Community BESS

The hourly net demand curves with community BESS for 8 May 2020, together with the SoC variations for each EC, are shown in Figure 13. The net-demand curves are obtained from a snapshot taken of the simulations carried out in Section 4.3. Therefore, the initial SoC for each EC is determined from the operation of the community BESS on the previous days. The initial SoC values for EC1 to EC5 are 20%, 45%, 79.2%, 58.2%, and 76.6%, respectively. One can immediately deduce that, for EC3 and EC5, the difference between the maximum SoC and the initial SoC significantly limits the capacity to reduce the reverse power flows for the considered day.

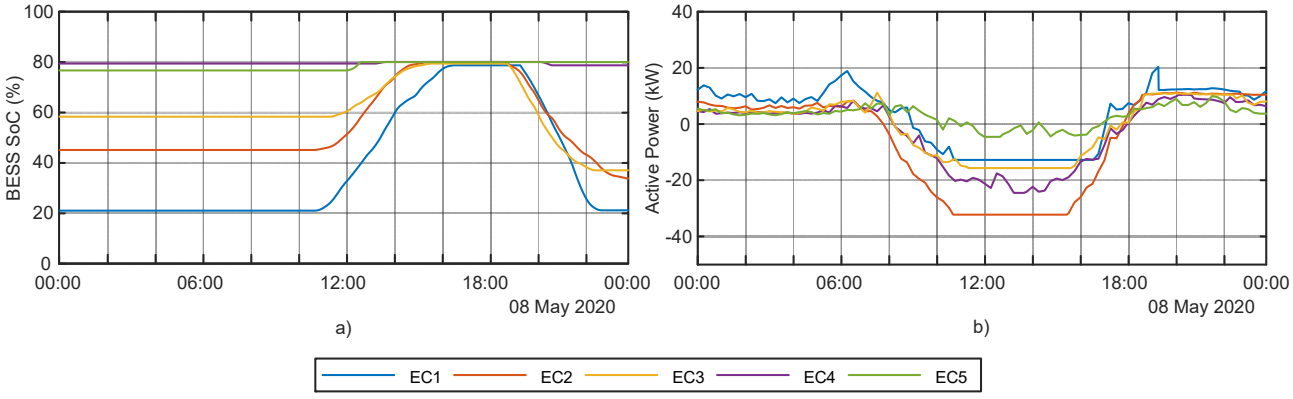

Figure 13. Net demand of the ECs with community storage for the selected case scenario. (**a**) The SoC variations of the BESS at the respective ECs. (**b**) The resulting net-demand at each EC.

Figure 13a shows the SoC variations for each BESS, whereby all of the community batteries reach the predefined limit of 80% during instances of reverse power flows. Figure 13b shows that EC2 has the highest reverse power of all the ECs, at −13.1 kW. For all of the ECs, the peak demands are limited to the predefined maximum power setpoints. An exception to this result occurs for EC1, where part of the peak demand is not compensated by the BESS as there was not enough capacity available. As expected, EC3 and EC5 showed small reductions in the reverse power flows due to the high initial SoC. These results clearly show that there is a compromise between the consumer's objective to maximizing self-consumption and the utility's objectives of maintaining a minimum base load and reducing the reverse power flows.

5.3. Impact of Communal BESS Placement on the EC Nodes

Simulations were then performed to verify the effect of the communal BESS placement on the voltage profile at each EC. Three case studies were simulated: (a) No communal BESS; (b) Communal BESS placed at the start of EC (substation secondary side); and (c) Communal BESS placed at the end of EC (furthest node from substation secondary side). Figure 14a shows a swarm plot of the phase (line-to-neutral) RMS voltages of all the nodes present in REC 1, at 15 min intervals throughout the day, without the communal BESS. From the figure, one can observe that there are overvoltage events due to the reverse power flow between 2:00 p.m. and 1:30 p.m. This corresponds to the period where solar PV generation reached a maximum. Violations of the 230 V +10% maximum limit were observed on multiple nodes in the REC.

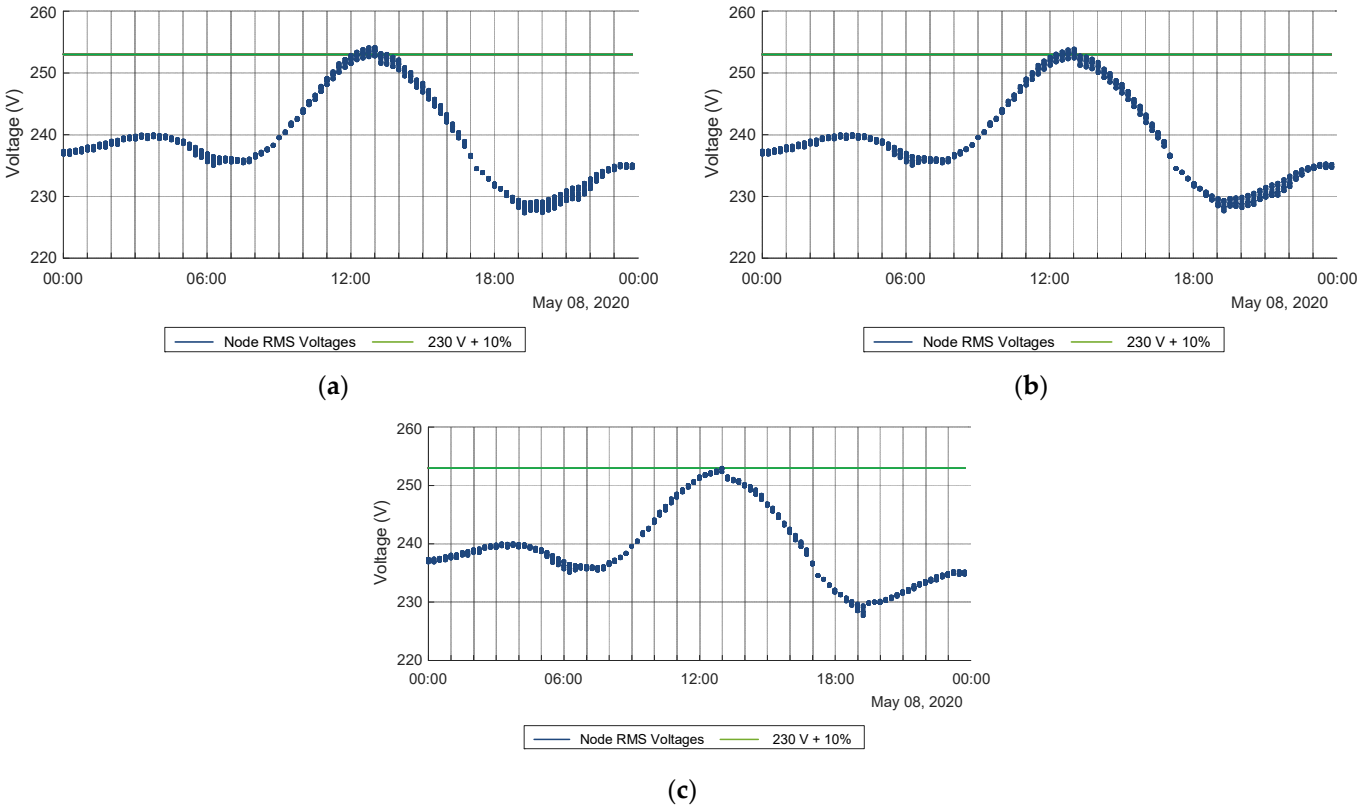

Figure 14. Swarm plot of the node phase voltages in REC 1 at 15-min intervals throughout the day. The green line represents the 230 V + 10% maximum limit (line-to-neutral). Each point is a resultant phase voltage at one of the nodes in the LV network. (**a**) No communal storage. (**b**) Communal storage placed at start of REC. (**c**) Communal Storage placed at the end of the REC.

Figure 14b shows a swarm plot of the phase (line-to-neutral) RMS voltages of all the nodes present in REC 1, at 15 min intervals throughout the day, with the communal BESS at the start of the REC. From the figure, one can observe that there are no significant changes in the voltage distributions over the whole day, as violations of the 230 V + 10% maximum limit were observed on multiple nodes in the REC. Figure 14c shows a swarm plot of the phase (line-to-neutral) RMS voltages of all the nodes present in REC 1, at 15 min intervals throughout the day, with the communal BESS at the end of the REC. From the figure, one can observe that there are reductions in the maximum voltages at the nodes, with violations of the 230 V + 10% maximum limit only occurring at 1 pm. In addition, there were also reduced voltage variations across all nodes in the network over the entire day (This is shown by smaller clusters in the swarm plot).

Similar plots were obtained for all five of the RECs and are not included here for the purpose of clarity. However, the resulting voltage variations at each node of the

five RECs that can be determined from these swarm plots are summarized in the bar graph of Figure 15. The horizontal line (purple) represents the 230 V + 10% maximum voltage limit for each of the five ECs. Without the communal BESS, this maximum voltage limit is exceeded in multiple nodes of nearly all of the ECs, with the exception of EC2. The most severe voltage magnitudes occurred in EC 3, where all the nodes exceeded the maximum voltage threshold. The resulting maximum voltages for EC1 to EC5 are 254.45 V, 253.25 V, 255.17 V, 253.75 V and 253.54 V, respectively. The minimum voltages that result during the peak power demand for EC1 to EC5 are 227.19 V, 228.87 V, 228.11 V, 228.23 V and 226.45 V, respectively.

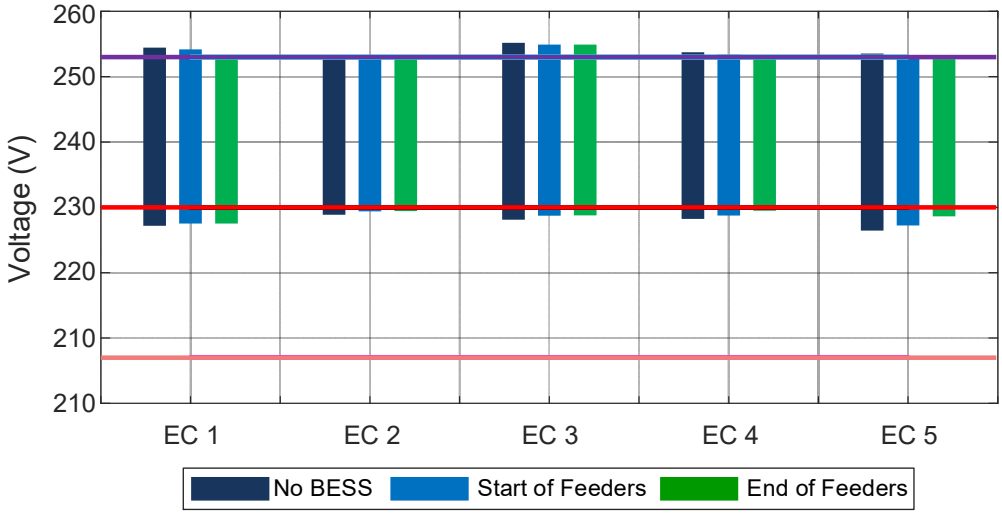

Figure 15. Bar graph of node voltage variations for each EC with and without the community BESS. The horizontal lines represent the 230 V ± 10% nominal voltage range for the Maltese LV network: Maximum limit (Purple), Nominal voltage (Red) and minimum voltage (Pink).

With the communal BESSs installed at the start of the EC, a reduction in the magnitude and duration of the reverse power flow at the substation was observed. EC 3 and EC 5 show the least reductions in reverse power flow as the initial SoC was close to the defined maximum threshold. in ECs where the initial SoC was low (e.g., EC 1 and EC 2), the operation of the communal BESS reduced the voltage magnitudes, however the maximum voltage limit was still exceeded in nearly all ECs, with the exception of EC 2. The resulting maximum voltages for EC1 to EC5 are 254.16 V (−0.14%), 253 V (−0.1%), 254.9 V (−0.11%), 253.37 V (−0.15%) and 253.05 V (−0.19%), respectively. Due to the reduction in power consumption during the peak demand, the minimum voltages for EC1 to EC5 increased to 227.51 V (+0.14%), 229.4 V (+0.23%), 228.71 V (+0.26%), 228.74 V (+0.22%) and 227.22 V (+0.34%), respectively.

With the communal BESSs installed at the end of the EC, the reductions in the magnitude and duration of the reverse power flow resulted in the lowest maximum voltages in the ECs. Similarly to the previous case scenario, EC 3 and EC 5 show the least reductions in reverse power flow as the initial SoC was close to the defined maximum threshold. in ECs where the initial SoC was low (e.g., EC 1 and EC 2), the operation of the communal BESS reduced the voltage magnitudes. In this scenario, the maximum voltage limit was only exceeded in EC 1 and EC 3. The resulting maximum voltages for EC1 to EC5 are 253.24 V (−0.48%), 252.76 V (−0.19%), 254.9 V (−0.11%), 252.9 V (−0.33%) and 252.67 V (−0.34%), respectively. Due to the reduction in power consumption during the peak demand, the minimum voltages for EC1 to EC5 increased to 227.53 V (+0.15%), 229.43 V (+0.25%), 228.77 V (+0.29%), 229.47 V (+0.54%) and 228.62 V (+0.96%), respectively.

6. Discussion

As mentioned in the previous sections, the challenges of achieving high penetrations of renewables in the Maltese distribution network, and in island power systems in general, should not be taken lightly. The formation of RECs provides an attractive solution to efficiently use any available assets by locally consuming the energy generated from renewables. The analysis for the five hypothetical RECs carried out in this study shows that, with the present penetration of renewables, the substation transformer sees an annual net-demand of 359.24 MWh, with the total reverse power injected in the grid amounting to 128.78 MWh. The maximum evening peak electricity demand at the transformer reaches 153 kW, while the reverse peak reaches a maximum of −125 kW. Deploying the energy storage units sized according to the BUF strategy ($BESS_{BUF}$) within the RECs resulted in a 7.95% reduction in the total energy demand from the grid during peak demand hours, and 16.9% reduction in the total energy supplied back to the grid during midday. The maximum evening peak electricity demand at the transformer was reduced to 78.2 kW, while the reverse peak reaches a maximum of −53.5 kW. Therefore, the installed PV capacity within the five RECs can be increased by up to 7.4% from the present installed capacity, while reaching the present reverse energy injection levels into the grid. This assumes a typical specific yield of 1626 kWh/kWp for PV systems in the Maltese islands [22].

By reducing their daily peak electricity demand and the reverse power flow into the utility grid, RECs can minimize their impact on the utility grid through increased self-sufficiency. The case study for a typical Maltese spring day showed that the communal BESS can also provide advantages within the same RECs. When installed at the end of the RECs, the communal BESS reduced the node rms voltages magnitudes by up to 0.48% by absorbing the reverse power flow. The degree of reduction in reverse power flow depends on the initial SoC of the batteries. Larger community storage systems could be deployed if additional ancillary services are provided to the grid in order to minimize the payback period and maximize profits. The ancillary services could include power quality improvement, regulation, and flexibility reserve.

Limitations

One should note that modelling assumptions were performed that might affect the results. As already mentioned in Section 3, most single-phase main meters in households where PV systems were installed did not have any logs for the exported active power. Therefore, the relationship between the PV generation and the exported active power for this study had to be analyzed and approximated for each individual consumer. This might affect the potential energy reductions for the modelled RECs.

Another assumption of this study concerns the controllability of the storage units within the REC. BESSs control the real power injection/absorption symmetrically on all three phases. However, in practice, all the three phases might not be available at the last node of the REC. An individual phase can directly feed several consumers as it is significantly cheaper to deploy single phase conductors than three phases (+neutral). In this context, only the partial load on that phase of the REC can be compensated by the BESS. Normally, there are no connections among phases (through power electronic converters) to allow for intra-phase power transfer. In addition, the charging/discharging rates must be limited to avoid overloading the conductors.

7. Conclusions

Renewable energy communities in the Maltese context can provide significant advantages to the citizens and the DSO. This study investigated the coordinated operation of the energy storage assets within the community, aiming at reducing the peak power exchanged between the REC and the main grid. Each LV feeder in the considered secondary substation was considered as an REC, such that RECs can be formed without the need to reconfigure the present distribution network. Each REC consists of different combinations of single-phase and three-phase consumers/prosumers. An analysis of the daily net-demand curves

for each REC revealed that oversupply occurs on more than 340 days for RECs 1 to 4, while for REC 5 oversupply occurs on 265 days. Community storage was proposed in this study as a means to reduce the peak power exchanged by each REC with the grid. The proposed sizing strategy for the community BESS is based on the battery utilization factor, which uses historical data for both demand and PV generation and ensures maximum utilization of the storage assets. The optimal sizes for the communal BESSs were determined to be of 57 kWh (EC 1), 55 kWh (EC 2), 31 kWh (EC 3), 37 kWh (EC 4) and 10 kWh (EC 5), respectively. Detailed analysis of the daily net-demand curves with and without storage for the each of the RECs showed reductions in the energy demand and reverse power flow during peak PV hours. The communal BESSs in the RECs are cycled nearly daily between the predefined SoC limits, except in certain periods of the year where the electricity demand is higher than the norm or when it is very close to the defined reference value.

Finally, power flow simulations were carried out on a typical spring day for two grid placement scenarios (start and end of the feeder, respectively). The impact of the communal BESS placement on the node voltages of all five energy communities was determined through a detailed analysis of the node phase rms voltages of each REC. The battery placement was seen to play a part in the benefits to the energy community itself. When the BESS was placed at the end of the EC, the voltage violations of the maximum limit were observed only for two communities out of the five modelled (EC 1 and EC 5), with resulting maximum voltages for EC1 to EC5 of 253.24 V (−0.48%), 252.76 V (−0.19%), 254.9 V (−0.11%), 252.9 V (−0.33%) and 252.67 V (−0.34%), respectively.

Author Contributions: Conceptualization, A.M.; methodology, A.M., C.S.S. and J.L.; software, A.M.; validation, C.S.S. and J.L.; formal analysis, A.M.; investigation, A.M., C.S.S. and J.L.; resources, A.M.; data curation, A.M.; writing—original draft preparation, A.M.; writing—review and editing, C.S.S. and J.L.; visualization, A.M.; project administration, A.M. and C.S.S. All authors have read and agreed to the published version of the manuscript.

Funding: This research was financed by the Energy and Water Agency under the National Strategy for Research and Innovation in Energy and Water (2021–2030), grant agreement reference number ESTELLE EWA 110/20/2/001-C.

Data Availability Statement: The original data used for the simulations are not publicly available.

Acknowledgments: The authors would like to acknowledge Enemalta PLC for providing the data required to conduct this study.

Conflicts of Interest: The authors declare no conflict of interest. The funders had no role in the design of the study; in the collection, analyses, or interpretation of data; in the writing of the manuscript, or in the decision to publish the results.

Nomenclature

BESS	Battery Energy Storage System
$BESS_{BUF}$	Battery Energy Storage System sized according to BUF
BUF	Battery Utilization Factor
CAPEX	Capital Expenditure
DSOs	Distribution System Operators
EC	Energy Community
EU	European Union
ICT	Information and Communications Technology
KPI	Key Performance Indicators
kWh	kilowatt-hours
LV	Low Voltage
MWh	megawatt-hours
P2P	Peer-to-Peer
PV	Photovoltaic

RECs	Renewable Energy Communities
SoC	State of Charge
TOU	Time-of-Use

References

1. EC Directive (EU) 2018/2001 of the European Parliament and of the Council of 11 December 2018 on the promotion of the use of energy from renewable sources. *Off. J. Eur. Union* **2018**, *L 328*, 82–209.
2. Menniti, D.; Pinnarelli, A.; Sorrentino, N.; Vizza, P.; Barone, G.; Brusco, G.; Mendicino, S.; Mendicino, L.; Polizzi, G. Enabling Technologies for Energy Communities: Some Experimental Use Cases. *Energies* **2022**, *15*, 6374. [CrossRef]
3. Di Silvestre, M.L.; Ippolito, M.G.; Sanseverino, E.R.; Sciumè, G.; Vasile, A. Energy self-consumers and renewable energy communities in Italy: New actors of the electric power systems. *Renew. Sustain. Energy Rev.* **2021**, *151*, 111565. [CrossRef]
4. Ceglia, F.; Esposito, P.; Faraudello, A.; Marrasso, E.; Rossi, P.; Sasso, M. An energy, environmental, management and economic analysis of energy efficient system towards renewable energy community: The case study of multi-purpose energy community. *J. Clean. Prod.* **2022**, *369*, 133269. [CrossRef]
5. Katsaprakakis, D.A.; Proka, A.; Zafirakis, D.; Damasiotis, M.; Kotsampopoulos, P.; Hatziargyriou, N.; Dakanali, E.; Arnaoutakis, G.; Xevgenos, D. Greek Islands' Energy Transition: From Lighthouse Projects to the Emergence of Energy Communities. *Energies* **2022**, *15*, 5996. [CrossRef]
6. O'Neill-Carrillo, E.; Mercado, E.; Luhring, O.; Jordan, I.; Irizarry-Rivera, A. Community Energy Projects in the Caribbean: Advancing Socio-Economic Development and Energy Transitions. *IEEE Technol. Soc. Mag.* **2019**, *38*, 44–55. [CrossRef]
7. Chamorro, H.R.; Yanine, F.F.; Peric, V.; Diaz-Casas, M.; Bressan, M.; Guerrero, J.M.; Sood, V.K.; Gonzalez-Longatt, F. Smart Renewable Energy Communities–Existing and Future Prospects. In Proceedings of the IEEE 22nd Workshop on Control and Modelling of Power Electronics (COMPEL), Cartagena, Colombia, 2–5 November 2021; pp. 1–6.
8. Felice, A.; Rakocevic, L.; Peeters, L.; Messagie, M.; Coosemans, T.; Camargo, L.R. Renewable energy communities: Do they have a business case in Flanders? *Appl. Energy* **2022**, *322*, 119419. [CrossRef]
9. Barone, G.; Buonomano, A.; Forzano, C.; Giuzio, G.F.; Palombo, A. Increasing renewable energy penetration and energy independence of island communities: A novel dynamic simulation approach for energy, economic, and environmental analysis, and optimization. *J. Clean. Prod.* **2021**, *311*, 127558. [CrossRef]
10. Doroudchi, E.; Khajeh, H.; Laaksonen, H. Increasing Self-Sufficiency of Energy Community by Common Thermal Energy Storage. *IEEE Access* **2022**, *10*, 85106–85113. [CrossRef]
11. Cielo, A.; Margiaria, P.; Lazzeroni, P.; Mariuzzo, I.; Repetto, M. Renewable Energy Communities business models under the 2020 Italian regulation. *J. Clean. Prod.* **2021**, *316*, 128217. [CrossRef]
12. Herenčić, L.; Kirac, M.; Keko, H.; Kuzle, I.; Rajšl, I. Automated energy sharing in MV and LV distribution grids within an energy community: A case for Croatian city of Križevci with a hybrid renewable system. *Renew. Energy* **2022**, *191*, 176–194. [CrossRef]
13. Dolatabadi, M.; Siano, P.; Soroudi, A. Assessing the Scalability and Privacy of Energy Communities by Using a Large-Scale Distributed and Parallel Real-Time Optimization. *IEEE Access* **2022**, *10*, 69771–69787. [CrossRef]
14. Zhu, H.; Ouahada, K.; Abu-Mahfouz, A.M. Peer-to-Peer Energy Trading in Smart Energy Communities: A Lyapunov-Based Energy Control and Trading System. *IEEE Access* **2022**, *10*, 42916–42932. [CrossRef]
15. Frisch, C.; Donohoo-Vallett, P.; Murphy, C.; Hodson, E.; Horner, N. An Electrified Nation: A Review of Study Scenarios and Future Analysis Needs for the United States. *IEEE Power Energy Mag.* **2018**, *16*, 90–98. [CrossRef]
16. Zhong, W.; Xie, K.; Liu, Y.; Yang, C.; Xie, S. Multi-resource allocation of shared energy storage: A distributed combinatorial auction approach. *IEEE Trans. Smart Grid* **2020**, *11*, 4105–4115. [CrossRef]
17. Aziz, M.; Dagdougui, H.; Elhallaoui, I. A Decentralized Game Theoretic Approach for Virtual Storage System Aggregation in a Residential Community. *IEEE Access* **2022**, *10*, 34846–34857. [CrossRef]
18. Sudhoff, R.; Schreck, S.; Thiem, S.; Niessen, S. Operating Renewable Energy Communities to Reduce Power Peaks in the Distribution Grid: An Analysis on Grid-Friendliness, Different Shares of Participants, and Economic Benefits. *Energies* **2022**, *15*, 5468. [CrossRef]
19. Regional, Geospatial, Energy and Transport Statistics Unit, Renewable Energy from Photovoltaic Panels: 2021. *Natl. Stat. Off. Malta Tech. Rep.* **2022**. Available online: https://nso.gov.mt/en/NewsReleases/Documents/2022/06/News2022106.pdf (accessed on 1 October 2022).
20. Micallef, A.; Spiteri Staines, C.; Cassar, A. Utility-Scale Storage Integration in the Maltese Medium-Voltage Distribution Network. *Energies* **2022**, *15*, 2724. [CrossRef]
21. Enemalta Corporation. The Network Code. Malta. 2013. Available online: https://www.enemalta.com.mt/wp-content/uploads/2018/05/Network-Code-EMC-Approved-October-2013-1.pdf (accessed on 1 October 2022).
22. Micallef, A.; Spiteri Staines, C. Generation Performance Analysis for Installed Photovoltaic Systems on the Maltese Islands. In Proceedings of the 1st Workshop on Blockchain for Renewables Integration (BLORIN 2022), Palermo, Italy, 2–3 September 2022.